International Journal of Multiphase Flow 36 (2010) 423–431

Contents lists available at ScienceDirect

International Journal of Multiphase Flow

journal homepage: www.elsevier.com/locate/ijmulflow

# Influence of the operation pressure on slug length in near horizontal gas–liquid pipe flow

U. Kadri *, R.F. Mudde, R.V.A. Oliemans

*Department of Multi-Scale Physics, Delft University of Technology, Prins Bernhardlaan 6, 2628 BW Delft, The Netherlands*

ARTICLE INFO

*Article history:*
Received 2 July 2009
Received in revised form 19 December 2009
Accepted 22 December 2009
Available online 4 January 2010

*Keywords:*
Gas–liquid pipe flow
Long slugs
Pressure
Operational failures

ABSTRACT

Slug flow is commonly observed in gas production offshore fields. At high operation pressure only short hydrodynamic slugs are observed. However, as the offshore fields become older, the operation pressure becomes lower and long slugs may form. At near atmospheric pressures the long slugs may reach a size of 500 pipe diameters or more. Such slugs can cause serious operational failures due to the strong fluctuating pressure. Identifying the operation pressure conditions at which the long slugs appear, may reduce or prevent these negative effects.

In this paper we process and analyse gas–liquid flow measurements in order to investigate the different slug types and their sensitivity to the operation pressure. The measurements were performed in a 103 m long pipe with an internal diameter of 0.069 m and an inclination of $-0.1^\circ$ from the horizontal. Three types of slugs were categorized according to the difference in liquid levels (liquid excess) between the slug front and tail. The long slugs were found to have the largest liquid excess after formation, whereas the hydrodynamic slugs had no liquid excess. The analysis of the measurements provides a detailed overview on the effect of pressure on the long slug length, and a safe operation region where long slugs will not appear.



## 1. Introduction

The cocurrent flow of gas and liquid in horizontal and near horizontal pipes results in a number of flow patterns. A *stratified flow* occurs at relatively low gas and liquid flow rates whereby the gas moves on top of the liquid. At higher rates of gas and liquid a *slug flow* pattern might exist where plugs of liquid move downstream separated by elongated bubbles moving along the top of the pipe. Although mostly short hydrodynamic slugs are observed, long slugs with sizes reaching 500 pipe diameters or more may form if the operation pressure becomes sufficiently low, e.g. in older gas production offshore fields. Such long slugs induce strong pressure fluctuations large enough to cause severe operational failures. Therefore, identifying the transition to the long slugs and the critical pressure at which they may appear, will be helpful in preventing or reducing such future operational failures.

Two main theoretical approaches are used to predict the transition from stratified to slug flow: stability of stratified flow and stability of slug flow. The *stability of stratified flow* was initially used by Hanratty and Hershman (1961) to describe waves on thin films over which air is blowing. A number of researchers Wallis and Dobbins (1973), Lin and Hanratty (1986) and Wu et al. (1987) followed this analysis to investigate the viscous long wavelength wave instability (VLW). The VLW theory successfully predicts that increasing the pipe size requires larger gas flow rates for the transition from stratified to slug flow in air–water horizontal pipe flow. The *stability of slug flow* considers the amount of liquid entering and leaving the slug. The slug becomes *neutrally stable*, not growing neither decaying, when a volumetric liquid balance is reached between the slug front and tail. This balance results in a minimum liquid area at the front, below it the slug becomes unstable (Bendiksen, 1984; Ruder et al., 1989; Woods and Hanratty, 1996).

Slug lengths have been reported to be in a range of 12–30*D* for horizontal air–water flow (Dukler and Hubbard, 1975; Nicholson et al., 1978; Nydal et al., 1992). This type of slugs is known as hydrodynamic. Kristiansen (2004) found a similar range of slug lengths for gas–liquid near horizontal pipe flow when introducing slugs at the inlet. However, when introducing stratified flow at the inlet he observed both short hydrodynamic and long slugs. Zoeteweij (2007) observed very long slugs reaching 500 pipe diameters. The long slugs form at relatively low gas and liquid velocities, where two sub-regimes are observed: neutrally stable, and growing slugs (Kadri et al., 2009).

In this paper we analyse measurements performed by Kristiansen (2004) in a 103 m long gas–liquid near horizontal pipe flow with an internal diameter of 0.069 m. The measurements were performed with air or high density gas at atmospheric and higher operation pressures. The analysis of the measurements is unique in the sense that it provides a simple mechanism for the appearance

* Corresponding author. Tel.: +31 27 83210; fax: +31 27 82838.
*E-mail address:* U.Kadri@tudelft.nl (U. Kadri).

0301-9322/$ - see front matter © 2009 Elsevier Ltd. All rights reserved.
doi:10.1016/j.ijmultiphaseflow.2009.12.006

of different slug types in the long slug regime. Slugs were categorized into three types according to the difference in liquid levels (*liquid excess*) between the front and tail: (1) slugs with large and initially constant excess; (2) slugs with decreasing excess; and (3) slugs with no excess. Slugs with large liquid excess can grow to become very long, whereas slugs that have no liquid excess are the shortest. We also found that small changes in the liquid excess, at the formation time, may result in large differences in slug length. Moreover, we identified the operation pressures at which the growing and stable slugs may appear.

A background on the theoretical approaches, stability of stratified flow and slug stability, is given in Section 2. Section 3 provides a description of the experimental facility and methods used for performing the measurements. A discrimination method between slug types is given in Section 4. In Section 5 we present results of the effect of slug types on the slug length at atmospheric and high operation pressures. Finally, the conclusions are presented in Section 6.

## 2. Background

### 2.1. Stratified flow pattern

An idealized model of the stratified flow pattern is represented by a simplified geometry. The diameter of the pipe is $D$. The height of the liquid layer along the centerline is $h_L$. The length of the segments of the pipe circumference in contact with the gas and liquid are $S_G$ and $S_L$, respectively. The length of the gas–water interface is denoted by $S_i$. The areas occupied by the gas and the liquid are $A_G$ and $A_L$, respectively. Given the pipe diameter, these parameters can be calculated, from measurements of $h_L$, by using geometric relations (e.g. Govier and Aziz, 1972). The momentum balances for the gas and the liquid flows are as follows:

$$-A_G\left[\left(\frac{dp}{dx}\right)+\rho_G g\cos\theta\left(\frac{dh_G}{dx}\right)\right]-\tau_{WG}S_G-\tau_i S_i+\rho_G A_G g\sin\theta=0, \quad (1)$$

$$-A_L\left[\left(\frac{dp}{dx}\right)+\rho_L g\cos\theta\left(\frac{dh_L}{dx}\right)\right]-\tau_{WL}S_L+\tau_i S_i+\rho_L A_L g\sin\theta=0, \quad (2)$$

where $\rho_G$ and $\rho_L$ are the gas and the liquid densities, $\theta$ is the inclination angle of the pipe from the horizontal, $dp/dx$ is the pressure gradient, $g$ is the acceleration due to gravity, and $dh_G/dx$ and $dh_L/dx$ are the gas and liquid hydraulic gradients, respectively. The time-averaged stress of the gas and liquid phases at the wall and the stress at the interface, $\tau_{WG}$, $\tau_{WL}$ and $\tau_i$, are defined in terms of friction factors, and calculated using the Blasius equation if $Re < 10^5$ and the wall roughness effect can be ignored, otherwise the Churchill equation is used (see Churchill, 1977). Due to the presence of waves at the interface, the interfacial friction factor becomes larger than the friction factor for a smooth surface. In this paper we use an estimation for the interfacial friction factor suggested by Hurlburt and Hanratty (2002). For given flow rates of liquid and gas Eqs. (1) and (2) are used to find the pressure gradient and the height of the liquid layer. However, these equations do not determine the stability of the stratified flow.

#### 2.1.1. Average liquid area

The average liquid area, $A_L = A_{L_{avg}}$, is calculated from the momentum balances for the stratified flow pattern, Eqs. (1) and (2). Substituting $A_L = A_{L_{avg}}$ and $A_G = A - A_{L_{avg}}$, Kadri et al. (2009) wrote Eq. (1) in the following form:

$$\left(\frac{dp}{dx}\right)=\frac{\tau_{WG}S_G-\tau_i S_i}{A-A_{L_{avg}}}+\rho_G g\sin\theta. \quad (3)$$

The average liquid area is the initial plane stratified flow in the pipe. This occurs when the pressure gradients of the two phases balance at the interface. Substituting Eq. (3) in Eq. (2) and assuming a fully developed horizontal pipe flow, Kadri et al. (2009) obtained a relation for $A_{L_{avg}}$ as follows:

$$A_{L_{avg}} = A\frac{\tau_{WL}S_L-\tau_i S_i}{\tau_{WL}S_L+\tau_{WG}S_G}. \quad (4)$$

The average liquid height $h_{L_{avg}}$ is calculated using Eq. (4) and geometric relations (e.g. Govier and Aziz, 1972). Eq. (4) successfully predicts the inverse proportionality between the gas flow rates and $h_{L_{avg}}$.

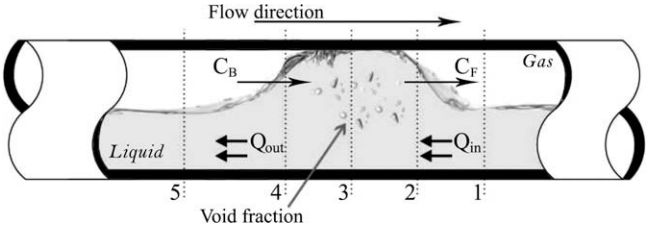


**Fig. 1.** Sketch of a slug.

### 2.2. Slug stability model

The slug stability model considers the rates of liquid entering or leaving the slug at its front or rear. Slugs are stable (not decaying) when the rates of liquid entering are not less than the rates leaving the slug. Fig. 1 gives an illustration of a slug moving with front velocity $C_F$ over a stratified liquid layer at station 1 of area $A_{L1}$ and actual velocity $u_1$. The volumetric flow rate of liquid entering the slug is

$$Q_{in} = (C_F - u_1)A_{L1}. \quad (5)$$

The rear of the slug is assumed to behave as a bubble moving with a velocity $C_B$. The volume fraction of the gas in the slug is $\varepsilon$. The volumetric flow rate of the liquid leaving the slug is

$$Q_{out} = (C_B - u_3)(1-\varepsilon)A \quad \text{at station 3}. \quad (6)$$

The parameter $u_3$ is the actual liquid velocity at station 3. Assuming neutral stability, $Q_{in} = Q_{out}$ and $C_F = C_B$, and making use of Eqs. (5) and (6), the following relation is obtained for the area of the stratified layer at the front:

$$\left(\frac{A_{L_1}}{A}\right)_{crit} = \frac{(C_B-u_3)(1-\varepsilon)}{(C_B-u_1)}. \quad (7)$$

Using Eq. (7) and geometric relations, the critical height, $h_{L_{crit}}$, at the slug front required for the slug to be neutrally stable is obtained. A detailed analysis of the slug stability model is well documented by Hurlburt and Hanratty (2002) and Soleimani and Hanratty (2003).

## 3. Experiments

The experiments analysed in this paper have been carried out by Kristiansen (2004) who investigated the transition from stratified to slug flow in multiphase pipe flow. The multiphase flow laboratory facility that was used is the SINTEF (The Foundation for Scientific and Industrial Research) flow loop located in Trondheim, Norway.

The flow loop was configured as an open loop when operating at atmospheric experiments, and as a closed system for experiments at higher pressures. The loop is 217 m long with 0.069 m internal diameter near horizontal pipe. A sketch of the experimental setup is given in Figs. 2 and 3 for open and closed loop configurations, respectively. The inlet is 114 m long adjusted with an inclination of $-1^\circ$ from the horizontal to ensure stratified flow at the inlet.

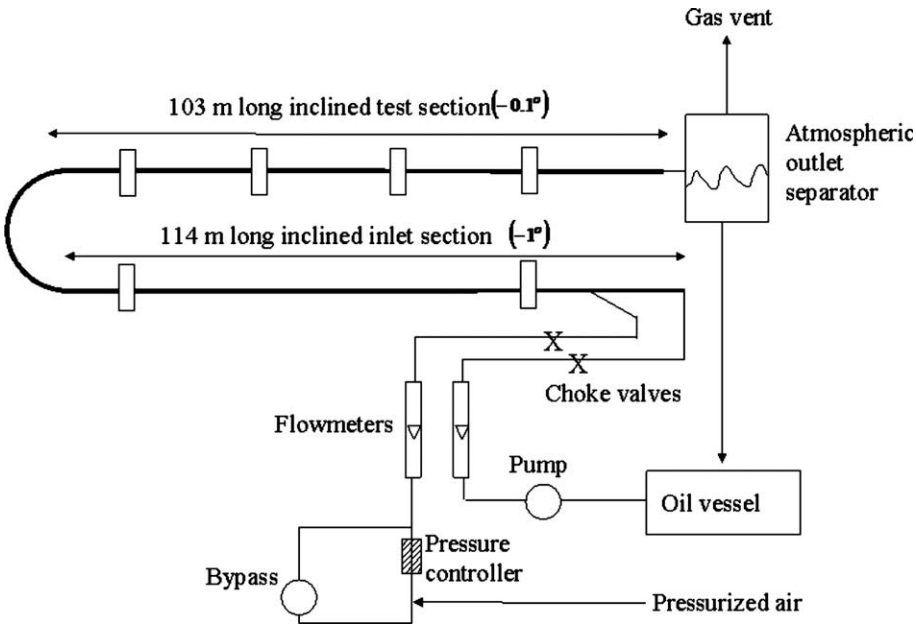


**Fig. 2.** Sketch of the SINTEF experimental setup for an open loop configuration.

The inlet ends in a 180° $u$-turn, and the last 103 m is the test section with an inclination of −0.1°. The geometry configuration of the flow loop is given in Fig. 4.

The fluids used in the experiments were air or Sulfur hexafluoride ($SF_6$) gas, and oil (*ExxsolD*80). Air was used when operating at atmospheric conditions, whereas $SF_6$ in higher pressure experiments. Sulfur hexafluoride ($SF_6$) is a dense gas with density approximately 5.5 times that of air, simulating high pressure conditions (natural gas up to 65 bar).

The liquid height was measured using 6 single-energy narrow-beam gamma densitometers, at locations: 19.4, 100, 128, 161, 182, and 200 m from the inlet (i.e. $L/D = 280,\ 1452,\ 1859,\ 2339,\ 2642$ and 2903, respectively). The gamma densitometers were calibrated using a two-point calibration in single-phase liquid and gas, respectively. The slug length was calculated at the sensors in the test section (last four sensors). Note that the slug length measurements presented in this paper are calculated at the last sensor downstream, where the development time is the largest.

The tests were performed in series with constant gas rate and increasing liquid rate, always starting as stratified flow. The full description of the test conditions can be found in Kristiansen (2004). A summary of the test conditions and fluids properties is shown in Table 1.

All measurements presented in this paper have been processed according to the different slug types presented in the next section. The processed measurements are addressed as "measurements".

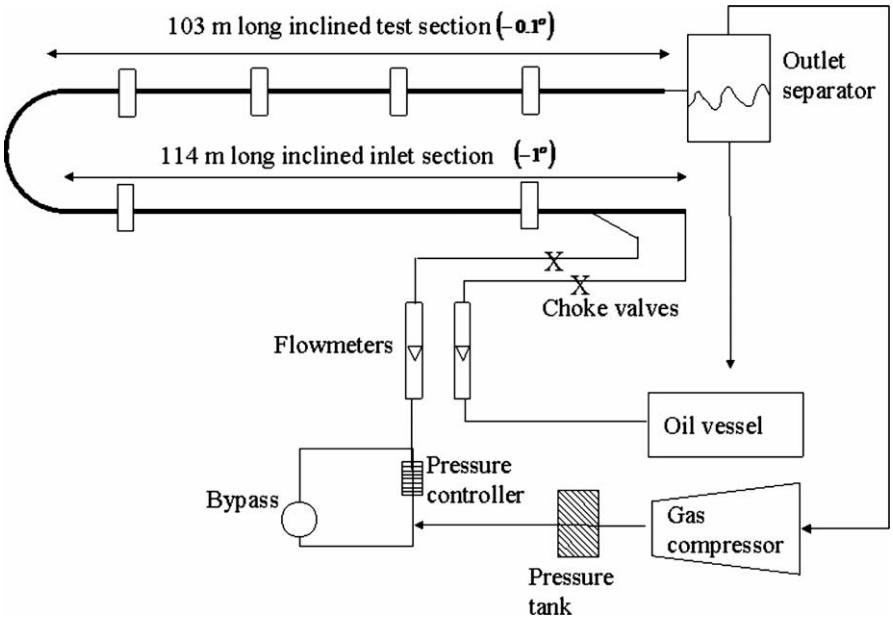


**Fig. 3.** Sketch of the SINTEF experimental setup for a closed loop configuration.

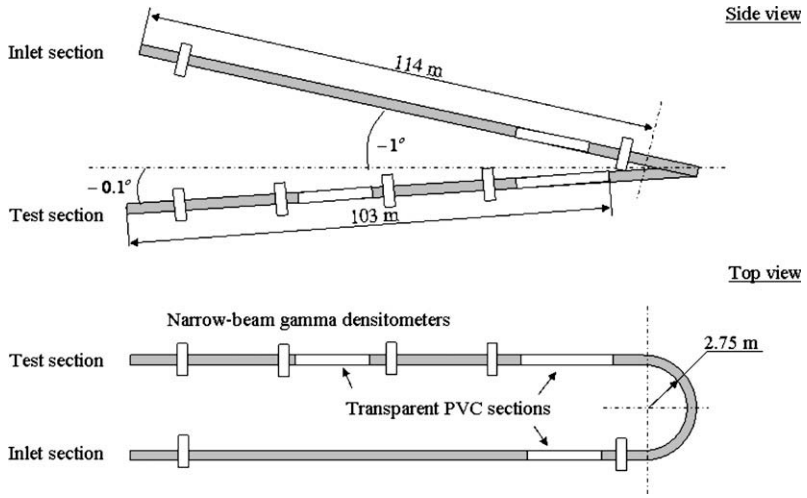


**Fig. 4.** Side and top views of the geometry configuration of the flow loop.

## 4. Definition of slug types by liquid excess

The slug formation is associated with liquid depletion at the tail of the slug (Woods and Hanratty, 1999). The slug becomes *neutrally stable*, neither growing nor decaying, when a volumetric balance between the liquid leaving, at the tail, and entering the slug, at the front, is reached. For a constant gas density and a continuous liquid phase, it can be shown from conservation of mass of the liquid phase that the liquid heights at the tail and front should be equal in order to reach neutral stability. That happens when the slug front approaches the tail of a second slug downstream, and the liquid excess becomes zero (i.e. that is why the first slug in the pipe can grow indefinitely).

**Table 1**
Summary of test conditions and fluid properties.

| | |
|---|---|
| Pipe diameter (m) | 0.069 |
| Pipe length (m) | 217.24 |
| Test section length (m) | 103 |
| Inlet section inclination (°) | −1 |
| Test section inclination (°) | −0.1 |
| Gas phase | Air or $SF_6$ gas |
| Liquid phase | *Exxsol*D80 oil |
| Gas density (kg/m$^3$) | 1.2, 9, 19, 46, 52 |
| Liquid density (kg/m$^3$) | 810 |
| Air viscosity (kg/ms) | $1.8 \times 10^{-5}$ |
| Gas ($SF_6$) viscosity (kg/ms) | $1.5 \times 10^{-5}$ |
| Liquid viscosity (kg/ms) | 0.0018 |
| Interfacial tension ($\sigma_{oil/air}$) (N/m) | 0.025 |
| Interfacial tension ($\sigma_{oil/SF_6}$) (N/m) | 0.021 |
| Pressure (bar a) | 1, 1.5, 3, 7, 8 |
| $U_{SG}$ (m/s) | 0.2–8 |
| $U_{SL}$ (m/s) | 0.05–0.5 |

### 4.1. Discrimination between slug types in measurements

Fig. 5 presents an example of time traces of three different slug types measured with the first sensor downstream of the initiation of each slug. Note that since Fig. 5 presents *time traces* of the liquid height measured at a fixed point, the front of each slug is on the left side of the slug (the information is moving from right to left). In Fig. 5a, the liquid height at the slug front is constant along a relatively large distance downstream, and remarkably higher than the liquid height at the tail. This observation indicates that such a slug is not influenced by the presence of a second slug (probably far) downstream. Such slugs are defined as *type I*. Slugs *type I* will keep

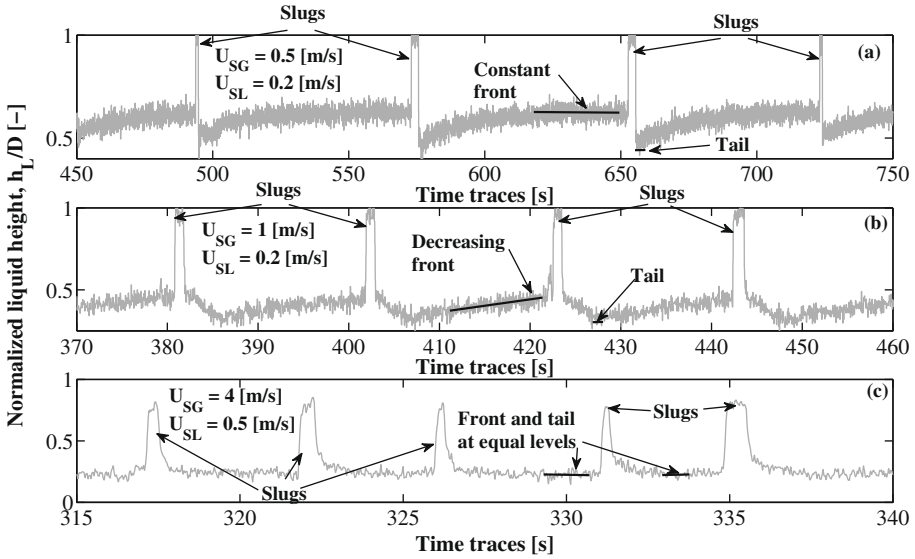


**Fig. 5.** Time traces of different slug types in $SF_6$ gas–oil pipe flow, $D = 0.069$ m, $\theta = -0.1°$, $P = 1.5$ bar a ($\rho_G = 9$ kg/m$^3$): (a) *type I*, (b) *type II*, and (c) *type III*.

growing until the front (which moves faster than the tail) approaches the tail of the next slug downstream. In Fig. 5b, the liquid height at the front decreases as a slug moves downstream. In this case, the slug growth is dependent on the downstream liquid depletion due to the existence of a second slug downstream. This type of slugs is defined as *type II*. In Fig. 5c, the liquid at the front and at the tail are equal, indicating a fully developed slug where the slug front approaches the tail of a second slug downstream. This type of slugs is denoted as *type III*.

The overall slug type of each measurement is denoted as one of the three types only if at least 90% of the individual slugs share the same type. Otherwise, the overall slug type is addressed as "undefined".

Note that the surface roughness increases with the gas flow rate. Thus, slugs *type I* develop on a smoother interface. This might be counterintuitive when looking at Fig. 5 due to the scale of the *x*-axis of each subplot.

### 4.2. Measurements of the liquid excess, $\Delta h_L$

In order to calculate the average liquid excess of the different slug types the following steps are made: (1) The time traces of the liquid height are examined at the first sensor where slugs are observed, at constant gas and liquid flow rates. (2) The average liquid height at the tail, $h_{L_{tail}}$, is calculated from the average height around the lowest point in the tail of each slug in the time traces. (3) The average liquid height at the front, $h_{L_{front}}$, is calculated from the average over a distance on the order of $10D$ from the front of all slugs in the time traces. (4) The average liquid excess of each measurement is calculated as follows:

$$\Delta h_L = h_{L_{front}} - h_{L_{tail}}. \tag{8}$$

### 4.3. Theoretical predictions of the liquid excess, $\Delta h_L$

#### 4.3.1. Slugs type I

At low gas and liquid flow rates, where the slug frequency is relatively low, a forming slug is far enough from a second slug downstream, as mentioned above. As a result, the liquid height at the front is not affected by the presence of the second slug. In this case, the liquid height at the front is the average height of the stratified flow, $h_{L_{front}} = h_{L_{avg}}$, whereas the liquid height at the tail is the minimum height calculated by slug stability ($h_{L_{tail}} = h_{L_{crit}}$). Therefore, the liquid excess of slugs *type I* is calculated as follows:

$$(\Delta h_L)_{typeI} = h_{L_{avg}} - h_{L_{crit}}, \tag{9}$$

where $h_{L_{avg}}$ and $h_{L_{crit}}$ are calculated from Eqs. (4) and (7), respectively. A comparison between the predicted and measured liquid heights is given in Fig. 6a.

#### 4.3.2. Slugs type II

Increasing the gas or liquid flow rates results in higher slug frequency (e.g. Gregory and Scott, 1969). At a sufficiently high frequency the liquid height at the front of the slug is affected by the presence of another slug downstream, so that the average liquid height at the front is lower than the initial height as presented in Fig. 6b. In this case, $\Delta h_L$ is approximated by the average height between $h_{L_{avg}}$ and $h_{L_{crit}}$ as follows:

$$(\Delta h_L)_{typeII} = \frac{h_{L_{avg}} - h_{L_{crit}}}{2}. \tag{10}$$

Eq. (10) presents an upper limit of $(\Delta h_L)_{typeII}$.

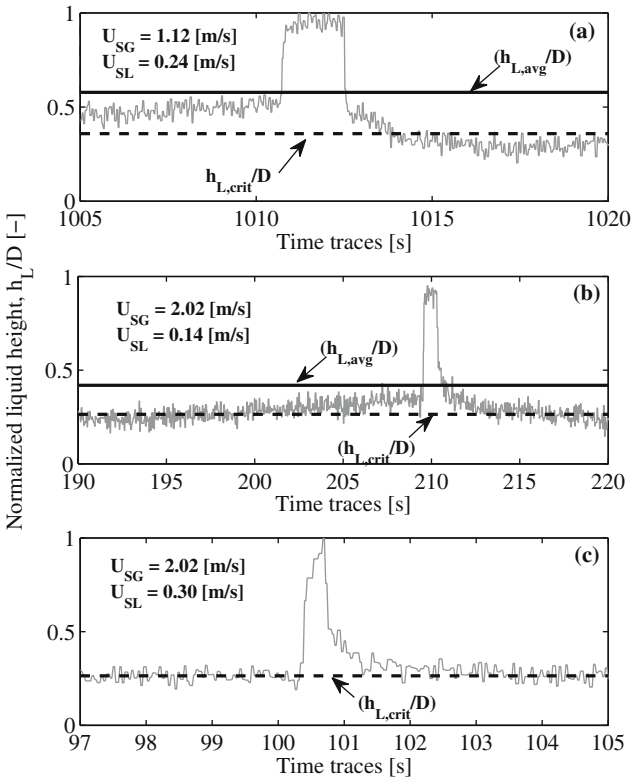


**Fig. 6.** Time traces of different slug types in air–oil pipe flow, $D = 0.069$ m, $\theta = -0.1^\circ$, $P = 1$ bar: (a) *type I*, (b) *type II*, and (c) *type III*. The experiments were performed by Kristiansen (2004).

#### 4.3.3. Slugs type III

Further increase of the flow rates results in the generation of a larger number of slugs. In this case, a forming slug reaches neutral stability immediately after formation. Thus, the liquid height at the front and tail are approximately the same (see Fig. 6c), thus:

$$(\Delta h_L)_{typeIII} = 0. \tag{11}$$

## 5. Results

In this section we compare theoretical predictions of the liquid excess, $\Delta h_L$, of the different slug types with (the processed) measurements. Additionally, we present a flow map and slug length measurements, at atmospheric and higher operation pressures, and identify the conditions at which the long slugs form.

### 5.1. Slug types and the normalized liquid excess, $\Delta h_L/D$

Fig. 7 compares $\Delta h_L/D$ of the three slug types at atmospheric pressure and different $U_{SG}$. The gas and liquid phases are air and oil (*ExxsolD*80), and the pipe diameter $D = 0.069$ m. Slugs *type I* are represented by filled triangles (▲), *type II* by circles (○), and *type III* by stars (*). The solid (-), dashed–dotted (- ·), and dashed (- -) lines are the theoretical predictions of $(\Delta h_L)_{typeI}$, $(\Delta h_L)_{typeII}$, and $(\Delta h_L)_{typeIII}$, calculated by Eqs. (9)–(11), respectively. The agreement between the theoretical predictions and measurements of the different slug types is satisfactory. However, Eq. (9) underpredicts and shows a wrong trend of $(\Delta h_L)_{typeI}$ at $U_{SG} < 1$ m/ s. This discrepancy is due to the undeveloped liquid height at the tail, which drops below $h_{L_{crit}}$ when a slug forms and, at low gas flow rates, slowly rebuilds to reach $h_{L_{crit}}$. This observation indicates a larger growth rate in slugs *type I* (due to the larger liquid excess) and a slower development (due to

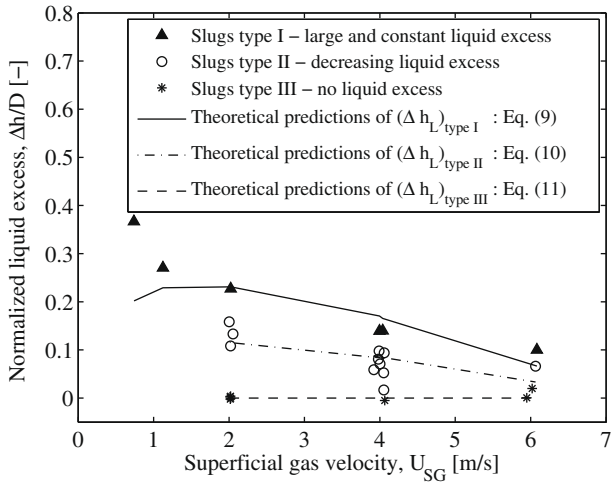


**Fig. 7.** Measurements and predictions of $\Delta h_L$ for the different slug types, in air–oil pipe flow, $D = 0.069$ m, $\theta = -0.1^\circ$, $P = 1$ bar. The data were derived from experiments done by Kristiansen (2004).

the lower flow rates). In the figure, we see that slugs *type I* have the largest liquid excess, *type III* have approximately zero excess, and the excess in *type II* is intermediate.

It is worth noting that the measurements presented in Fig. 7 were performed at different $U_{SL}$. At constant $U_{SG}$, slugs *type I* have the lowest $U_{SL}$, whereas slugs *type III* have the largest. The flow rates flow map is further discussed in the next sub-section.

### 5.2. The length of the different slug types at atmospheric pressure

Dukler et al. (1985) proposed a model in which a relation between the minimum stable slug length and the Reynolds number in the slug was obtained. Based on the model by Dukler et al. (1985), a stable slug (i.e. not decaying) has an initial minimum length of $8D < L_S < 16D$, for the range of flow conditions presented in this paper. At relatively high gas and liquid flow rates, each two neighbouring slugs may collide and double their lengths (e.g. Kristiansen, 2004). Since the slug is moving at velocities larger than the downstream liquid it absorbs any liquid excess between the slug tail and front. This is the key difference between the three types. A slug *type III* becomes neutrally stable immediately after formation, so that it can only grow by collision between slugs reaching, on average, a length of $16D < L_S < 32D$. However, slugs *type I* and *type II* will grow further until the tail of the next slug downstream is approached, where $\Delta h_L = 0$ and $C_F = C_B$ are satisfied.

Woods and Hanratty (1999) defined sub-regimes in the slug flow regime based on the Froude number $Fr = u_L/\sqrt{gh_L}$ and the location of slug formation. They claimed that slugs that form within a distance of $40D$ from the inlet are dependent on the design of the inlet. These slugs, form at supercritical flow conditions ($Fr > 1$), and have a maximum initial length of $40D$. In this paper, we define $L_S = 40D$ as the transition from short hydrodynamic to long slugs (Zoeteweij, 2007). The sub-plots in Fig. 8 show a flow map (on the left) and slug length measurements (on the right) in air–oil near horizontal pipe flow at atmospheric operation pressure. The transition between the short hydrodynamic and the long slugs is presented by the gray bold-solid line. The dashed line (–) is the predictions by slug stability model for the transition from stratified to slug flow. In Fig. 8, we obtain that only slugs *type I* have grown to become long ($L_S > 40D$). Slugs *type II* are mostly larger than slugs *type III*. However, both types are hydrodynamic ($L_S < 40D$). In the flow map, we also find that slugs *type I* (the only long slugs here) are found at relatively small $U_{SG}$ and $U_{SL}$. This observation is in agreement with the detailed measurements and theoretical calculations of the long slug regime by Kadri et al. (2009).

### 5.3. The length of the different slug types at $P = 1.5$ bar a ($\rho_G = 9$ kg/m$^3$)

In Fig. 9, the gas phase is $SF_6$ at the operation pressure $P = 1.5$ bar a (the effective density, $\rho_G = 9$ kg/m$^3$, simulates an operating pressure of 12 bar). In the slug length measurements (on the right) we notice that all slugs *type I* are long, as in the atmospheric case in Fig. 8. However, part of the slugs *type II* are also long, unlike the atmospheric case. On the other hand, all slugs *type III* are short. It is worth noting that slugs *type III* may double their length when two slugs collide and merge as a single slug. It is also remarkable, that the long slugs *type II* differ fundamentally from the long slugs *type I*. Long slugs *type II* form at flow rates large enough to create large waves downstream. The growth of the long slugs *type II* involves collisions with these large waves.

An interesting observation was found at measurements of similar flow rates but with a small difference in the initial liquid excess that resulted in large differences in the final slug length. As an example, in the flow map of Fig. 9 there are two measurements at $U_{SL} = 0.17$ m/s, and $U_{SG} = 1$ m/s denoted as $M1$ and $M2$, where $(\Delta h_L)_{M1}$ is 3% larger than $(\Delta h_L)_{M2}$. Although the difference between $(\Delta h_L)_{M1}$ and $(\Delta h_L)_{M2}$ is relatively small, the difference of the final

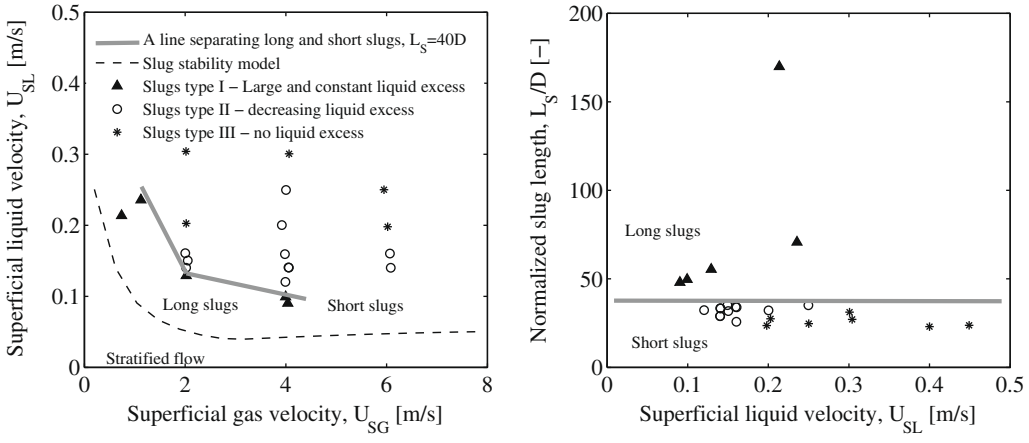


**Fig. 8.** Flow regime transition data for different $U_{SL}$ (on the left) and $L_S/D$ (on the right) in air–oil pipe flow, $D = 0.069$ m, $\theta = -0.1^\circ$, $P = 1$ bar. The data were derived from experiments done by Kristiansen (2004).

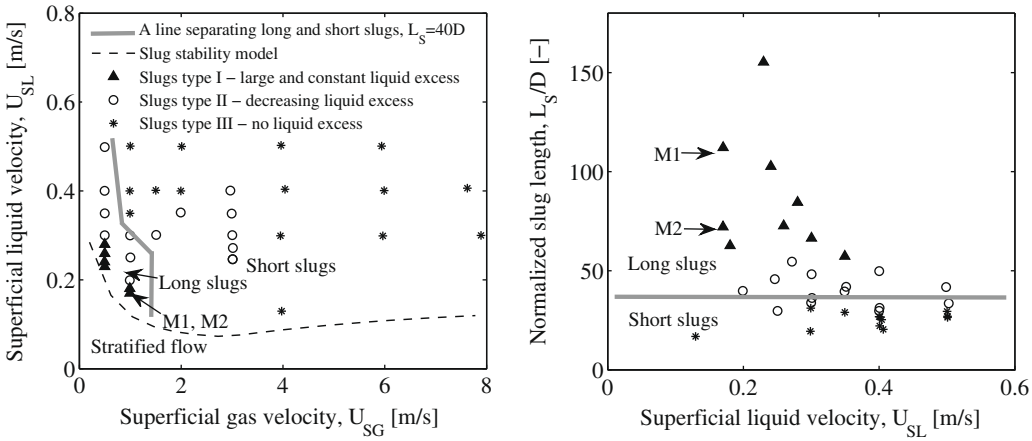


**Fig. 9.** Flow regime transition data for different $U_{SL}$ (on the left) and $L_S/D$ (on the right) in $SF_6$ gas–oil pipe flow, $D = 0.069$ m, $\theta = -0.1°$, $P = 1.5$ bar a (the effective density, $\rho_G = 9$ kg/m$^3$, simulates an operating pressure of 12 bar). The data were derived from experiments done by Kristiansen (2004).

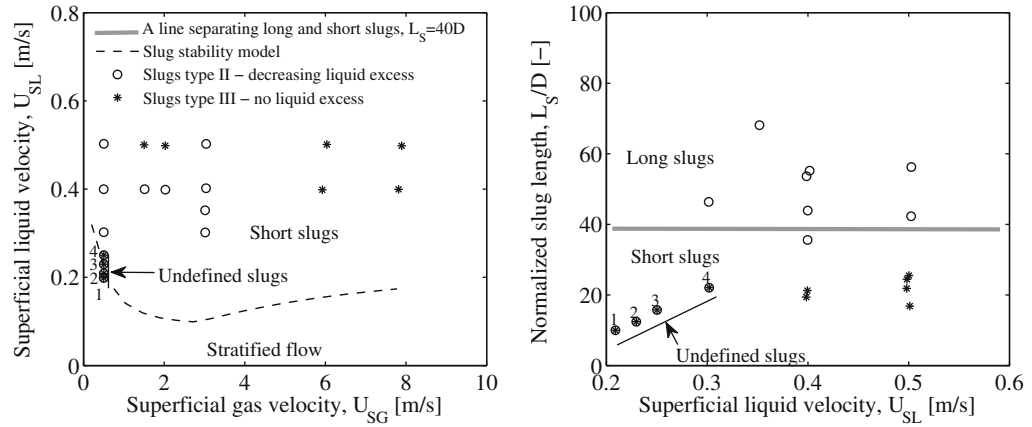


**Fig. 10.** Flow regime transition data for different $U_{SL}$ (on the left) and $L_S/D$ (on the right) in $SF_6$ gas–oil pipe flow, $D = 0.069$ m, $\theta = -0.1°$, $P = 3$ bar a (the effective density, $\rho_G = 18.5$ kg/m$^3$, simulates an operating pressure of 23 bar). The data were derived from experiments done by Kristiansen (2004).

slug length in the two measurements is remarkably large: $(L_S/D)_{M1} = 112$, whereas $(L_S/D)_{M2} = 72$.

### 5.4. The length of the different slug types at $P = 3$ bar a ($\rho_G = 18.5$ kg/m$^3$)

Operating at higher pressure results in higher critical flow rates and $h_{L_{crit}}$ required for the transition to slug flow (Eq. (7)), on the one hand, and lower flow rates and $h_{L_{avg}}$ of the stratified flow (Eqs. (1), (2) and (4)), on the other hand. As a results, the slug flow region "shrinks". This shrinkage can be seen by comparing the flow maps presented in Figs. 9 and 10.

In the flow map of Fig. 10, we find that increasing the operation pressure, $P = 3$ bar a (the effective density, $\rho_G = 18.5$ kg/m$^3$, simulates an operating pressure of 23 bar), results in the appearance of slugs only at higher $U_{SL}$, as shown in the flow map. In this set of measurements no slugs *type I* were observed in the same measurements, and all long slugs are *type II* with lengths that do not exceed 70*D*. At low flow rates, slugs *type II* and *type III*, and waves were observed, simultaneously. Such slug measurements, at which multiple slug types appeared, were indicated as "undefined slugs" in Fig. 10. Time traces of these slugs show the combination of slugs *type II*, *type III*, and large waves, as presented in Fig. 11. These slugs form close to the inlet (of the test section) and propagate at relatively low velocities. As a result, the slugs are being formed within, relatively, small distances, leading to a larger slug frequency compared with that of the long slugs. In addition, increasing $U_{SL}$ results,

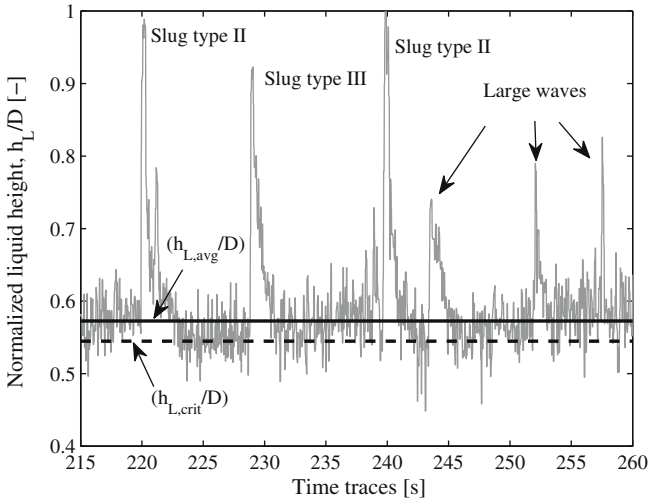


**Fig. 11.** Time traces of $SF_6$ gas–oil pipe flow, $D = 0.069$ m, $\theta = -0.1°$, $P = 3$ bar a (the effective density, $\rho_G = 18.5$ kg/m$^3$, simulates an operating pressure of 23 bar). The experiments were performed by Kristiansen (2004).

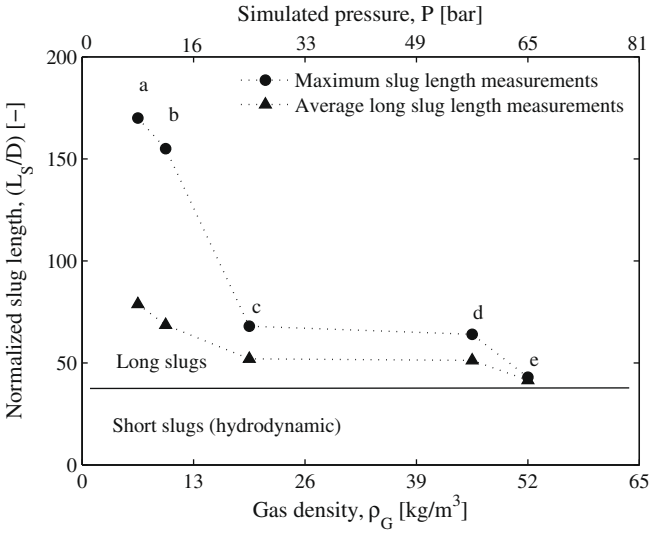


**Fig. 12.** Largest and average (long slugs) normalized slug length, $(L_S/D)_{max}$, as function of gas density and simulated pressure in gas–liquid pipe flow, $D = 0.069$ m, $\theta = -0.1°$. The data were derived from experiments done by Kristiansen (2004).

contrary to slugs *type I*, in increasing $L_S$ (see slug numbers in Fig. 10).

### 5.5. Effect of pressure on the long slugs – summary

Fig. 12 summarizes the effect of pressure on the presence of the long slugs in the pipe. In the figure, the bullets (•) represent measurements of the maximum slug length in the pipe at the given flow conditions, whereas the filled triangles (▲) represent the average length of the long slugs. For a gas density of air at atmospheric and near atmospheric operation pressures, the long slugs (a and b) are the longest in the long slug region ($L_S > 150D$). On the other hand, at gas density $18.5 < \rho_G < 52$ kg/m$^3$ simulating operation pressure of $23 < P < 65$ bar, the long slugs are neutrally stable and their length did not exceed $L_S = 70D$. Above $\rho_G = 52$ kg/m$^3$ ($P > 65$ bar), no long slugs have been observed.

From Figs. 8–10 and 12 we conclude that the average slug length decreases when increasing the operation pressure, at constant $U_{SG}$ and $U_{SL}$. This conclusion is in agreement with findings by Ujang et al. (2006), who examined the pressure effect on the slug frequency at flow conditions and a pipe diameter similar to these presented in this paper. Ujang et al. (2006) reported that the slug frequency is not sensitive to a change in the operation pressure. When increasing the operating pressure $\Delta h_L$ decreases (Eqs. (4) and (7)), and since the slug frequency remains constant the slug length has to decrease in order to conserve the liquid mass.

## 6. Conclusions

(1) Slug flow measurements have been analysed in order to investigate the sub-regimes in the long slug regime, and the effect of pressure on the appearance of the long slugs.
(2) Slugs have been categorized into three types according to the liquid excess between the front and tail: (1) *type I* – slugs that are unaffected by the presence of other slugs downstream. They have relatively large and constant initial liquid excess. Due to the large liquid excess, this type of slugs may become extremely long $O(100D)$; (2) *type II* – slugs moving over a depleted liquid layer due to the passage of other slugs. Thus, these slugs have a decreasing liquid excess. Depending on the flow conditions, the length of this type of slugs varies from short hydrodynamic to long; and (3) *type III* – fully developed slugs with no liquid excess. These slugs are the shortest, being 8–16$D$ long at low flow rates, but double their lengths at larger flow rates due to collisions and merging with other slugs.
(3) Theoretical predictions by stratified and slug stability models correctly predict $\Delta h_L$ of the different slug types. However, the models underpredict $(\Delta h_L)_{typeI}$ at $U_{SG} < 1$ m/s.
(4) At atmospheric pressure, the long slugs were found to be *type I*. When increasing the liquid flow rates, the frequency of slugs *type I* increases, and neutral stability is reached earlier in the pipe, due to the presence of a larger number of slugs. As a result, the slug length decreases.
(5) Increasing the operation pressure results, on one hand, in larger flow rates that are required for the transition from stratified to slug flow. On the other hand, the stratified liquid height decreases (due to the larger gas density), and slugs become neutrally stable earlier. As a result, slugs become shorter and the long slug sub-regime "shrinks".
(6) Slugs *type II* may also become long ($L_S > 40D$). However, the mechanism behind their growth is related to the collision and absorption of large waves travelling downstream.
(7) Slugs *type I* have not been observed at $\rho_G \geqslant 18.5$ kg/m$^3$ ($P \geqslant 23$ bar). At $18.5 < \rho_G < 46$ kg/m$^3$ ($23 < P < 65$ bar) the long slugs were only *type II*, neutrally stable at the outlet, with lengths less than 70$D$. At $\rho_G = 52$ kg/m$^3$ ($P = 65$ bar) only short hydrodynamic slugs (*type III*) were found.
(8) Slight changes in the liquid excess can lead to large difference in the final slug length, and thus slug frequency.

## Acknowledgments

The authors wish to thank Dr. Olav Kristiansen for providing his full data from his PhD in order to allow the detailed analysis. This research is a part of the research project: "Long liquid slugs in stratified gas/liquid flow in horizontal and slightly inclined tubes", sponsored by STW (Dutch Foundation for Technological Research).

## References

Bendiksen, K.H., 1984. An experimental investigation of the motion of long bubbles in inclined tubes. Int. J. Multiphase Flow 10, 467–483.
Churchill, S.W., 1977. Friction-factor equation spans all fluid-flow regimes. Chem. Eng. 7, 91.
Dukler, A.E., Hubbard, M.G., 1975. A model for gas–liquid slug flow in horizontal tubes. Ind. Eng. Chem. Fundam. 14, 337–347.
Dukler, A.E., Maron, D.M., Brauner, N., 1985. A physical model for predicting the minimum stable slug length. Chem. Eng. Sci. 40, 1379–1385.
Govier, G.W., Aziz, K., 1972. The Flow of Complex Mixtures in Pipes. Van Nostrand Reinhold Co., NY. p. 563.
Gregory, G.A., Scott, D.S., 1969. Correlation of liquid slug velocity and frequency in horizontal cocurrent gas–liquid slug flow. AIChE J. 15, 933–935.
Hanratty, T.J., Hershman, A., 1961. Initiation of roll waves. AIChE J. 7, 488–497.
Hurlburt, E.T., Hanratty, T.J., 2002. Prediction of the transition from stratified to slug and plug flow for long pipes. Int. J. Multiphase Flows 28, 707–729.
Kadri, U., Zoeteweij, M.L., Mudde, R.F., Oliemans, R.V.A., 2009. A growth model for dynamic slugs in gas–liquid horizontal pipes. Int. J. Multiphase Flow 35, 439–449.
Kristiansen, O., 2004. Experiments on the transition from stratified to slug flow in multiphase pipe flow. Ph.D. thesis, Norwegian University of Science and Technology (NTNU), Trondheim.
Lin, P.Y., Hanratty, T.J., 1986. Prediction of the initiation of slugs with linear stability theory. Int. J. Multiphase Flow 12, 79–98.
Nicholson, M.K., Aziz, K., Gregory, G.A., 1978. Intermittent two phase flow in horizontal pipes: predictive models. Can. J. Chem. Eng. 56, 653–663.
Nydal, O.J., Pintus, S., Andreussi, P., 1992. Statistical characterization of slug flow in horizontal pipes. Int. J. Multiphase Flow 18, 439–453.
Ruder, Z., Hanratty, P.J., Hanratty, T.J., 1989. Necessary conditions for the existence of stable slugs. Int. J. Multiphase Flow 15, 209–226.
Soleimani, A., Hanratty, T.J., 2003. Critical liquid flows for the transition from the pseudo-slug and stratified patterns to slug flow. Int. J. Multiphase Flow 29, 51–67.
Ujang, P.M., Lawrence, C.J., Hale, C.P., Hewitt, G.F., 2006. Slug initiation and evolution in two-phase horizontal flow. Int. J. Multiphase Flow 32, 527–552.

Wallis, G.B., Dobbins, J.E., 1973. The onset of slugging in horizontal stratified air–water flow. Int. J. Multiphase Flow 1, 173–193.
Woods, B.D., Hanratty, T.J., 1996. Relation of slug stability to shedding rate. Int. J. Multiphase Flow 22, 809–828.
Woods, B.D., Hanratty, T.J., 1999. Influence of Froude number on physical processes determining frequency of slugging in horizontal gas–liquid flows. Int. J. Multiphase Flow 25, 1195–1223.
Wu, H.L., Pots, B.F.M., Hollenberg, J.F., Meerhoff, R., 1987. Flow pattern transitions in two-phase gas/condinsate flow at high pressure in an 8-inch horizontal pipe. In: Proc. BHRA Conf., The Hague, The Netherlands, pp. 13–21.
Zoeteweij, M.L., 2007. Long liquid slugs in horizontal tubes. Development study and characterization with electrical conductance techniques. Ph.D. thesis, Delft University of Technology, Department of Multi-Scale Physics, Delft, The Netherlands.